All Sciences Proceedings

1st International Conference on Recent and Innovative Results in Engineering and Technology

August 16-18, 2023 : Konya, Turkey

ICRIRET

All Sciences Proceedings
http://as-proceeding.com/

https://as-proceeding.com/index.php/icriret

CFD Study on the Hydrodynamics of a Submarine Model Operating Near a Free-Surface

Taner Cosgun*[1], Yavuz Hakan Ozdemir [2]

[1]*Department of Naval Architecture and Marine Engineering, Yildiz Technical University, Turkey*
[2]*Department of Motor Vehicles and Transportation Technologies, Canakkale Onsekiz Mart University*

**(tcosgun@yildiz.edu.tr)*

Abstract – This paper investigates the hydrodynamic performance of a model scale submarine operating near the free surface using Computational Fluid Dynamics. The RANS approach has been adopted to model the flow around the submerged body. The resistance predictions of the submarine model validated against available experimental data, and then the variation of the acting forces on the submarine was investigated in a constant submergence depth. The results were presented in terms of drag coefficient, flow field visualizations and the free surface deformations, for the better understanding of the hydrodynamics of the submarine at near surface operation.

Keywords – Submarine, Free-Surface, CFD, Resistance, DARPA

I. INTRODUCTION

The conventional submarines periodically need to operate in close proximity of the free surface for a while for the purpose of the fresh air intake and the battery charging with the aid of diesel generators. Furthermore, surface observation and the communication operations also require to be close to the surface. When the submarine approach through the free surface, hull starts to interact with the free surface and these interactions cause significant changes on the hydrodynamics of the submarine.

Many researchers have studied the free surface effects on underwater vehicles. Domiciano et al. [1] estimated the wave resistance of a submarine at the snorkel submergence using Boundary Element Method. They have reported the wave resistance component and the free surface deformations for a range of velocities and submergence depths. Sulisetyono and Yulianto [2] adopted thin ship theory to predict the wave making resistance of a mini-submarine. Moonesun et al. [3] numerically modelled a model scale submarine at surface condition. They revealed the wave profile, the deck flooding and the additional frictional resistance of the body for different Froude Numbers using Computational Fluid Dynamics (CFD). Wilson-Haffenden [4] applied CFD and EFD techniques to investigate the resistance of a submarine travelling below the free surface. In their experimental investigation, Moonesun et al.[5] analyzed the hull resistance of the submarine model at surface condition and snorkel depth. Sarraf et al. [6] performed experimental and numerical investigation of a new design bluff submarine. They have tested different geometries under several scenarios to understand the behaviour of squad submarines and to determine the optimal body geometry. Ling et al. [7] conducted a numerical study to examine the hydrodynamics of the DARPA suboff under free surface effect. Ling et al. [8] used CFD to investigate the effect of length-to-diameter ratio on the performance of a submarine operating near the free surface. Dogrul [9] studied the hydrodynamics of a submarine moving close to a free surface. They revealed the influence of the different submergence rates and velocities on the performance of the body.

The present paper covers the numerical modelling of a submarine moving close to the free surface. The resistance and the flow field around the submarine is examined in a constant submergence rate. The velocity and pressure field around the body, free surface deformations and the total drag variations are presented.

II. Materials and Method

The computations are carried out on the benchmark submarine model introduced by the Defence Advanced Research Projects Agency (DARPA) [10]. The DARPA AFF-8 submarine hull form is shown in Fig.1 and the main dimensions of the model are presented in Table 1.

Fig. 1 The geometry of the DARPA AAF-8 submarine form

Table 1. The main dimensions of the submarine model

LOA (m)	4.356
LBP (m)	4.261
Dmax (m)	0.508
S (m2)	6.348
∇	0.706

The submergence depth (H) of the submarine was determined as the length between the centerline of the body and the free-surface. In this study, a constant submergence depth equal to H/D=1.5 was investigated.

A commercial CFD tool, Star ccm+ is utilized in the computations. The solver implements finite volume method to discrete the governing equations. The numerical solution of the time-dependent Navier-Stokes equations along with the continuity equation was conducted to calculate the velocity and pressure fields. The equations are:

$$\frac{\partial u_i}{\partial x_i} = 0 \qquad (1)$$

$$\rho\left(\frac{\partial u_i}{\partial t} + u_j \frac{\partial u_i}{\partial x_j}\right) = -\frac{\partial p}{\partial x_i} + \frac{\partial}{\partial x_j}\left(\mu \frac{\partial u_i}{\partial x_j} - \rho\overline{u_i' u_j'}\right) \qquad (2)$$

Where u_i is the time-averaged velocity, p is the pressure, ρ is the density and μ is the dynamic viscosity. Last term on the right hand side of the Eq.2 donates the Reynolds stress tensor. Realizable k-ε turbulence model with a wall-function approach is used to model the turbulent field. Details about the turbulence model can be found in the solver's documentation [11].

Flow around the submarine model was solved using a rectangular-shaped computational domain. Numerical predictions were performed in a Cartesian coordinate system with the negative –x axis in the direction of incoming flow. The submarine model was placed at the $2L_{BP}$ and $5L_{BP}$ away from the inlet outlet boundaries, respectively. Sidewalls of the solution domain were extended to the length of $2L_{BP}$ from the centre of the submarine hull. A uniform velocity profile which is equal to V=3.051 m/s was imposed to the inlet boundary of the solution domain.

Unstructured hexahedral grid elements was used to construct the solution domain. General view of the grid structure is given in Fig.2.

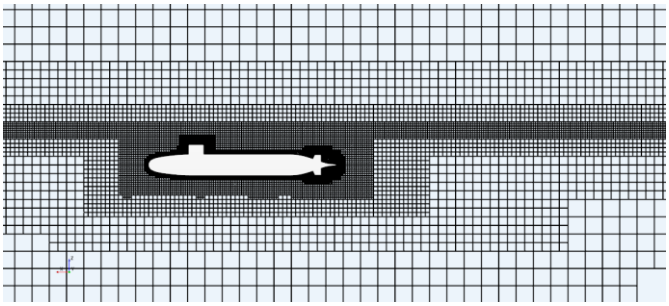

Fig. 2 The grid structure around the submarine hull

While generating the surface grid along the submarine body, the y+ values are kept in the range of 30<y+< 300 on the submarine hull to satisfy the wall function approach of the RANS closure ($y+ = u_\tau y/\nu$, where u_τ is the friction velocity, y is the height of the first cell on the wall and ν is the kinematic viscosity). A couple of refinement regions were created at some parts of the solution domain. First, computational grid was refined around the submarine hull. Furthermore,

local grid refinements were applied to the wake region and the appendages.

III. NUMERICAL RESULTS

The numerical modelling of the flow around the submarine model was performed using computational fluid dynamics. At first, the DARPA model was simulated in deep water conditions and the numerical predictions were validated against the measurements of Liu and Huang [12]. Then, the calculations were repeated for near free-surface scenario. The total resistance coefficients (C_T) of both two cases are presented in Table 2. All calculations were carried out for V=3.051 m/s.

Table 2. Total resistance coefficients

	CFD, Deep Water	EFD, Deep Water	CFD, H/D=1.5
C_T	104.1	102.3	174.5

As shown in Table 2, the numerical predictions of the total resistance in deep water condition is very close to the experimental data. When the submarine operates in near free-surface condition, the resistance significantly increases. To understand the variation of the forces near the free surface, the flow field around the submarine was examined.

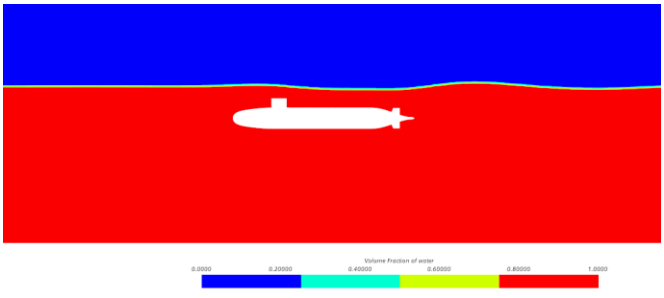

Fig. 3 The free surface elevation at the midsection of the hull

Fig. 3 shows the free surface elevation at H/D=1.5. When the submarine moves close to the free-surface, it generates a wave field on the still water. The first wave crest occurs near the bow region, while the location of the wave trough seems to be near the aft of the hull. The creation of the wave field means there is an additional wave drag acting on the submarine. As expected, the total resistance force in near free-surface condition increases due to the wave drag, which is not exist in deep water operation.

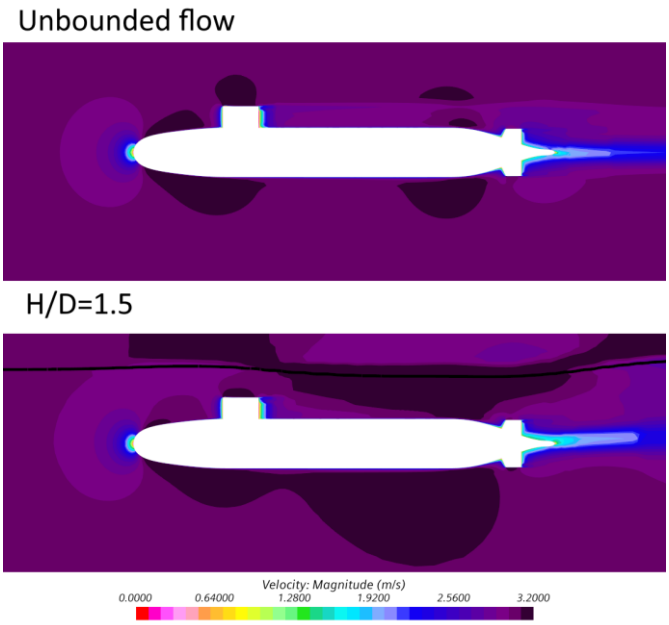

Fig. 4 The velocity field around the submarine

The velocity field around the submarine at deep water and near free-surface conditions are presented in Fig.4. The flow field in bow region interacts with the free surface, when the body moves close to the water surface. These interactions are also seen at the aft region. Furthermore, the velocity field in wake at H/D=1.5 is highly asymmetric compared to those of deep water (unbounded flow).

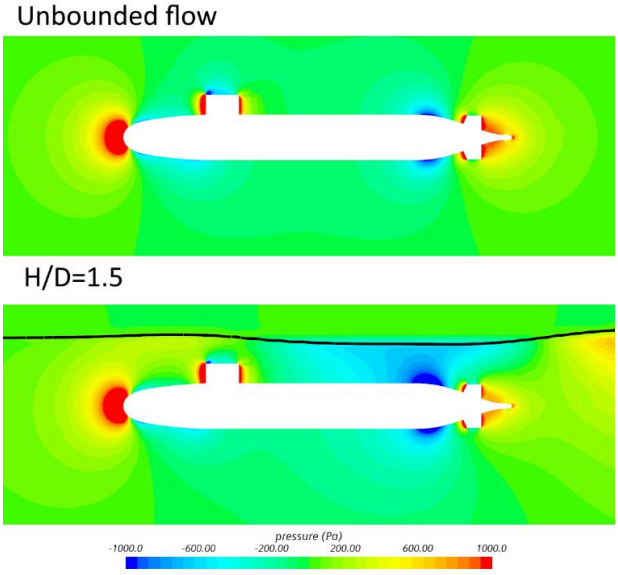

Fig. 5 The pressure field around the submarine

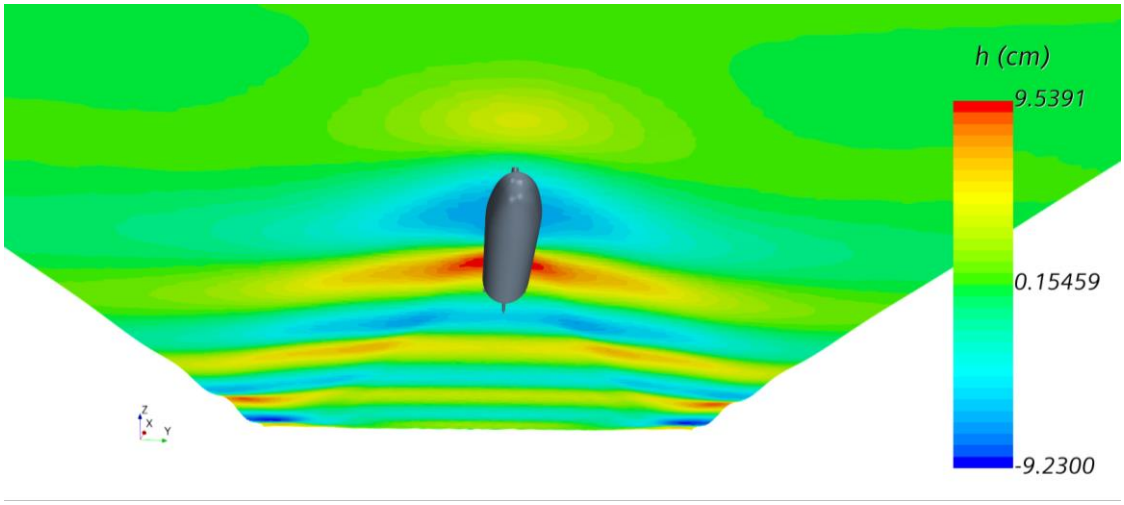

Fig. 6 The wave field around the hull

Fig. 5 shows the pressure field around the submarine. The same free surface interactions as seen in the velocity field are also appear in the pressure field. The high pressure region at the bow is symmetric in deep water condition. On the other hand, when the submarine moves close to the free surface, the pressure zone interacts with the water surface, and causes the wave elevation. Besides, the wave trough coincides with the low pressure zone at the aft region of the body.

The general view of free surface deformations around the submarine is given in Fig.6. The wave elevation at the bow region of the submarine creates a diverging wave field. Even though there is no free surface piercing body, the generated wave field seems to be in the form of Kelvin waves.

IV. CONCLUSION

The flow around the submarine operating near a free surface is modelled with the aid of computational fluid dynamics. The resistance and the free surface deformations of well-known DARPA submarine model was computed at shallow submergence condition. The results show that, when the body operates near the free-surface, the pressure field around the hull interacts with the water surface and causes the wave elevations. This wave elevations induce a wave drag on the submarine, and increase the total resistance. The increment of the total resistance at the calculated case is nearly 70%. The crest and trough of the first wave is coincides at the high and low pressure zones at the bow and aft regions, respectively. Furthermore, the near free surface operation of the body generates a diverging wave field in the form of Kelvin waves.

REFERENCES

[1] V. Domiciano, M. B. de Conti, and A. L. Silvestre Nunes, “Submarines Wave Resistance At Snorkel Submergence,” in The Twenty-second International Offshore and Polar Engineering Conference, 2012.

[2] A. Sulisetyono and A. Nugroho Yulianto, “The wave making resistance prediction of a mini-submarine by using tent function method,” MATEC Web Conf., vol. 177, Jul. 2018.

[3] M. Moonesun, H. Dalayeli, M. Javadi, S. H. Mousavizadegan, A. Ursalov, and A. Gharachahi, “Wave profile and deck wetness of submarine at surface condition,” nternational J. Recent Adv. Multidiscip. Res., vol. 2, no. 12, 2015.

[4] S. Wilson-Haffenden, M. Renilson, D. Ranmuthugala, and E. Dawson, “An Investigation into the Wave Making Resistance of a Submarine Travelling below the Free Surface,” in International Maritime Conference 2010: Maritime Industry, 2010.

[5] M. Moonesun et al., “Technical Notes on the Near Surface Experiments of Submerged Submarine,” Int. J. Marit. Technol., vol. 5, 2016.

[6] S. Sarraf, M. Abbaspour, K. M. Dolatshahi, S. Sarraf, and M. Sani, “Experimental and numerical investigation of squat submarines hydrodynamic performances,” Ocean Eng., vol. 266, p. 112849, Dec. 2022.

[7] X. Ling, Z. Leong, C. Chin, and M. Woodward, “Free Surface Effect on the Hydrodynamics of an Underwater Vehicle Hullform, the Darpa Suboff,” Int. J. Marit. Eng., vol. 164, 2022.

[8] X. Ling, Z. Q. Leong, and J. Duffy, “Effects of length-to-diameter ratio on a near free surface underwater vehicle,” in Applied Ocean Research, 2023, vol. 138, p. 103657.

[9] A. Doğrul, “Hydrodynamic Investigation of a Submarine Moving Under Free Surface,” J. ETA Marit. Sci., vol. 7, no. 3, pp. 212–227, 2019.
[10] [N. C. Groves, T. T. Huang, and M. S. Chang, “Geometric Characteristics of DARPA Suboff Models (DTRC Model Nos. 5470 and 5471) (No. DTRC/SHD-1298–01),” 1989.
[11] Siemens, “Star-CCM+ User Guide version 14.02.” 2019.
[12] H.-L. Liu and T. T. Huang, “Summary of DARPA Suboff Experimental Program Data (No. CRDKNSWC/HD-1298-11),” Jun. 1998.